THE INSTITUTE OF PAPER CHEMISTRY

Appleton, Wisconsin

BEHAVIOR OF FIBROUS AND NONFIBROUS COMPONENTS IN THE CORRUGATING OPERATION

PART III. A STUDY OF THE DYNAMICS OF THE UPPER CORRUGATING ROLL--PRELIMINARY REPORT

Project 1108-22

Report Three

A Progress Report

to

FOURDRINIER KRAFT BOARD INSTITUTE, INC.

March 23, 1961

TABLE OF CONTENTS

THE INSTITUTE OF PAPER CHEMISTRY

Appleton, Wisconsin

BEHAVIOR OF FIBROUS AND NONFIBROUS COMPONENTS IN THE CORRUGATING OPERATION

PART III. A STUDY OF THE DYNAMICS OF THE UPPER CORRUGATING ROLL--PRELIMINARY REPORT

SUMMARY

As a part of a comprehensive study of the mechanics of corrugating and the behavior of the fibrous and nonfibrous materials during corrugating, an investigation of the dynamics of the upper roll has been initiated. It is known that, in addition to rotary motion, the upper roll exhibits linear motion parallel to a line joining the centers of the upper and lower corrugating rolls. This linear motion, which has been termed "jumping" or "drop action," is a result of the rolling action of mating corrugations of the two rolls and is accommodated in corrugator design by permitting the upper roll bearing assembly to slide on guide rods.

The rotary and linear motions of the upper corrugating roll are pertinent to the flute molding process because the forces which cause these motions are exerted by the lower corrugating roll and act transversely through the medium at and near the center of the corrugating labyrinth. A tangential force overcomes the resistance (inertia and friction) of the upper roll to rotary motion during constant or changing corrugating speeds. A radial force drives the upper roll in its "jumping" motion. The tangential and radial forces taken together comprise a resultant force exerted by the lower roll through the medium and thereby constitute the molding force in corrugating.

Molding is one of several significant phases of the corrugating operation, whereby the medium acquires a permanent set and retains a fluted shape while the liners are adhered.

It may be appreciated, therefore, that a study of the motions of the upper corrugating roll and the forces causing those motions should lead to a better understanding of the stresses and strains induced in the medium during molding. A study of this type complements a previous study of the stresses and strains associated with the process of forming the flutes, the latter process occurring at an earlier stage in the passage of the medium through the labyrinth. Moreover, it is conceivable that variations in the degree of roll jump or rotary motion due to speed or other factors may cause variations in the molding of the flutes. Variations in molding force may be related to high-lows and/or leaning flutes in the corrugated board, inasmuch as an improperly molded flute may spring back upon leaving the labyrinth and retain thereafter a distorted shape. Furthermore, variations in molding force may affect (a) the stress relief which is believed to occur in the medium near the zone of transverse compression, and (b) the side wall strength; thus, molding force may also be related to runnability, in the sense of medium rupture.

A theoretical analysis was made of the linear and rotary motion of the upper roll. Regarding linear motion, equations were derived that relate the mass and linear acceleration of the upper roll to the forces acting on it. These forces are (a) radial (molding) force exerted by the lower roll transversely through the medium, (b) weight of the upper roll,

(c) force of sliding friction between the upper roll bearing assemblies and their guide rods, and (d) hydraulic loading of the upper roll.

Similarly, the rotary motion was expressed in terms of roll inertia, angular acceleration, tangential molding force, bearing friction and web tension.

The experimental phase of this preliminary study was devoted primarily to a study of the linear motion of the upper roll on the assumption that it has the dominant effect on molding force. Roll weight and force of sliding friction were estimated with reasonable confidence from the machine design of one of the Institute's experimental corrugators equipped with A-flute rolls. Special instrumentation was devised to measure instantaneously the hydraulic force acting at one bearing assembly of the upper roll. The hydraulic force is demonstrably variable, depending on the instantaneous position of the upper roll along its line of motion, and exhibits the characteristics of a mechanical spring. The instantaneous hydraulic force measurement during corrugating was displayed on a dual-beam oscilloscope as a curve of force vs. time, along with a curve of roll displacement vs. time as measured by a displacement transducer inserted between the shoulders at one end of the two corrugating rolls. Photographs of the force-time and displacement-time curves were obtained while corrugating a 26-lb. semichemical medium at 40, 100 and 300 ft./min. and also with bare rolls at 40 ft./min.

A typical linear motion of the upper corrugating roll during the formation of one A-flute was as follows: the upper roll moved away from the lower roll twice during the formation of each flute, reaching the apex of

its outward movement each time an arch was molded at the center of the labyrinth. The upper corrugating roll came nearest the lower roll when the side walls of the flute were at the center of the labyrinth, that is, twice for each flute.

Maximum linear accelerations of the upper roll occurred at the arches and side walls of the flute because at these instants the upper roll reversed its direction of motion. These peak accelerations were calculated graphically from the displacement vs. time curves. It was found that the peak linear accelerations of the roll increased approximately as the square of the corrugating speed. This characteristic is typical of a common class of mechanical oscillations and, therefore, lends greater confidence to the graphical determinations of acceleration.

The estimates of peak acceleration and the measurements of instantaneous hydraulic force permitted calculation of the radial component of the molding force that acts on the arches and side walls of the flute. Although the experimentation was not extensive, there was an apparent trend for the radial molding force to decrease at the arches and to increase at the side walls with increase in corrugating speed. From this trend it may be inferred that the molding of the A-flute arches became less complete at increased corrugating speed, and the side walls more severely stressed at the higher speed.

The above-mentioned trend of change in molding force with change in speed was confirmed by measurement of the change in residual caliper of the medium in the tips of flutes taken from single-faced board which had been fabricated at two different corrugating speeds. Measurements of residual caliper

at the side walls verified the molding force trend in the case of B-flute but not in A-flute.

It was found that the force on the side walls of the roll corrugations was substantially larger when the rolls were run bare at 40 f.p.m. than when corrugating a medium at the same speed. This result is in apparent agreement with the practice of operators to run the corrugator bare at only very low speeds to avoid damaging the rolls.

An estimate of the tangential driving force was obtained from measurements of rotary bearing friction at very low speed. This estimate of driving force is appropriate to corrugating at constant speed except that it does not account for possible momentary angular accelerations or decelerations of duration comparable to the period of forming one flute and which may arise from conjugate action of the roll corrugations (in conjunction with the medium) or from the lower roll drive system. In general, the tangential force was two orders of magnitude lower than the radial force, indicating that the molding force was essentially equal to the radial component and directed along the line of roll centers. However, considering the trend to decreased radial molding force at the arches as speed is increased, it may be expected that the total molding force would become more highly dependent on its tangential component and would be inclined away from the line of roll centers.

The present data and the noted trends should be viewed only as preliminary data because of the small sampling during this phase of the

investigation. The results indicate, however, that this type of experimental and analytical approach is feasible and offers promise as a method of studying the molding forces during corrugating.

Work is now in progress on an improved experimental technique which utilizes an accelerometer transducer instead of a displacement transducer. This substitution will afford direct recording of acceleration with a consequent saving of analysis time and presumably an increase in accuracy. Furthermore, it should be possible to sample a substantial number of consecutive flutes during corrugating and also in the fabricated single-faced board and thereby perhaps relate molding forces to the high-low and leaning flute phenomena and runnability. Instrumentation is also being installed at both ends of the upper corrugating roll for the purpose of obtaining a more complete and accurate record of roll motion.

Reviewing the results of this study, the following salient points may be noted:

1. A theoretical analysis was made of the molding force of corrugating, in terms of the rotary and linear motion of the upper corrugating roll.

2. An experimental investigation of the linear motion of the upper roll of the Institute research corrugator yielded estimates of the magnitude of the molding force acting on the arches and side walls of the flute.

3. Although the experimentation was not extensive, the data indicated that an increase in corrugating speed reduced the molding force at the arches of the flute and increased the force at the side wall. Measurements of medium caliper after corrugating partially confirmed this trend.

4. Variation in molding force with increase in corrugating speed possibly may be related to high-low and leaning flutes (because of lack of adequate molding of the arches) and to runnability (because of lack of stress relief or because of maceration of the flute side walls).

5. Work currently in progress is directed to improving the accuracy and efficiency of the experimental method of determining molding force.

6. It is believed that this type of investigation is capable of determining whether variations in molding force (due to machine design and operation and/or medium properties) are related to (a) high-low flutes, (b) leaning flutes and (c) runnability.

INTRODUCTION

The Institute of Paper Chemistry, on behalf of the Fourdrinier Kraft Board Institute, has been pursuing a fundamental study of the mechanics of corrugating and the behavior of the fibrous and nonfibrous components in the corrugating operation. One of the goals of this study is to gain a better understanding of the relationship between the physical properties of the medium and its behavior during corrugating in terms of runnability, ability to mold and bond, and the occurrence of high-low and leaning flutes.

An earlier phase of this study was concerned with an exploratory analysis of the stresses and strains which are induced in the medium from the time it leaves the parent roll at the stand until the flute is formed--that is, to a point just preceding the center point of the corrugating rolls (1). It was concluded that flute formation probably involves both the bending and shear properties of the corrugating medium and that the coefficient of friction may be a significant factor in runnability. In the aforementioned study, a distinction was made between the "forming" process and the subsequent "molding" process, the latter taking place near and at the center point of the labyrinth when substantial transverse compression stresses are brought to bear on the medium. The nature of the transverse molding stresses was not analyzed in Reference (1).

Germane to the consideration of molding stresses is a well-recognized phenomenon of corrugating wherein the upper corrugating roll possesses not only rotary motion but also translational motion parallel to a line joining the centers of the upper and lower corrugating rolls. This "up and down"

motion of the upper roll has been called "drop action" and was described by Wilson (2) several years ago. Concurrent with the writing of this report, work of Peters (3) has been published which draws attention to the same phenomenon and terms it "jumping" of the upper roll, amounting to four to eight ten-thousandths of an inch. Peters discusses qualitatively the possible effect on the corrugating medium. Extensive measurement of the magnitude of this aspect of upper roll motion has been made in connection with a study at the Institute of the relationship between roll clearances and flute height (4).

The significance of the jumping action to molding stresses is that the force which drives the upper roll in its upward motion is provided by the lower roll acting through the medium, that is, the driving force is the molding force. More exactly, the force which drives the roll upward is the radial component of the total molding force; the other component is the tangential force exerted by the bottom roll in driving the upper roll in rotary motion. Inasmuch as the jumping motion of the upper roll is oscillatory in nature, the radial driving force is not constant. Therefore, it is not quite proper to speak of the molding force, in the sense of a constant force related only to the hydraulic loading on the corrugator rolls, but rather the driving force (molding force) which continually varies in a manner corresponding to the roll motion.

It appears reasonable that variations in the degree of roll jumping (for whatever reasons there may be) will cause corresponding variations in the molding forces. Inasmuch as corrugating, in its simplest

concepts, consists of inducing a permanent set in the medium so it will retain a fluted shape, it follows that variations in the intensity of the molding forces may be expected to permit varying degrees of "spring-back" of the flute arches when the medium leaves the labyrinth. Such variations in spring-back may be contributory to high-lows and/or leaning flutes. Moreover, it is believed that the transverse compression during molding offers some relief of the tension stress and strain in elements of the medium immediately preceding the zone of transverse compression, because of the Poisson expansion in the machine direction of the medium. Variations in the degree of tension relief (due to variations in the molding force) may be a factor in whether or not the medium fractures in the late stages of forming.

A study was undertaken, therefore, of the dynamics of the upper corrugating roll and its relationship to machine design and the properties of the medium. This report describes an exploratory theoretical and experimental phase of a study of the motion of the upper roll.

THEORETICAL CONSIDERATIONS

The forces which may be expected to act on the upper roll of the Institute experimental corrugator (shown in Fig. 1) and which are pertinent, therefore, to the motion of the upper roll are diagrammed in Fig. 2. In the latter illustration the upper corrugating roll and its bearing assembly are denoted by the solid-line circle and the lower corrugating roll is represented by the dashed-line circle. The bearing assembly of the lower roll is rigidly fixed to the frame of the corrugator, but the upper roll and its bearing assembly can move parallel to the center line shown in Fig. 2.

The lower roll exerts a force, F, on the upper roll, of which one vector component, T, directed tangentially, provides the motive force to rotate the upper roll, and the other vector component, R, directed radially, causes the upper roll to move along the line of roll centers. The force F, is of interest to the analysis of corrugating because this force acts transversely through the corrugating medium while the latter is at the center of the labyrinth of the corrugating rolls. Accordingly, the force F is involved in the process of molding the medium into its fluted shape. It should be emphasized that F is a force, not a stress. The distribution of this force over one or more teeth at and near the center of the labyrinth is probably nonuniform with respect to both time and location on the tooth profile.

Inasmuch as one component of the molding force F causes rotary motion and the other component causes translational motion (jumping) of the roll, it is appropriate to consider these two types of motions independently

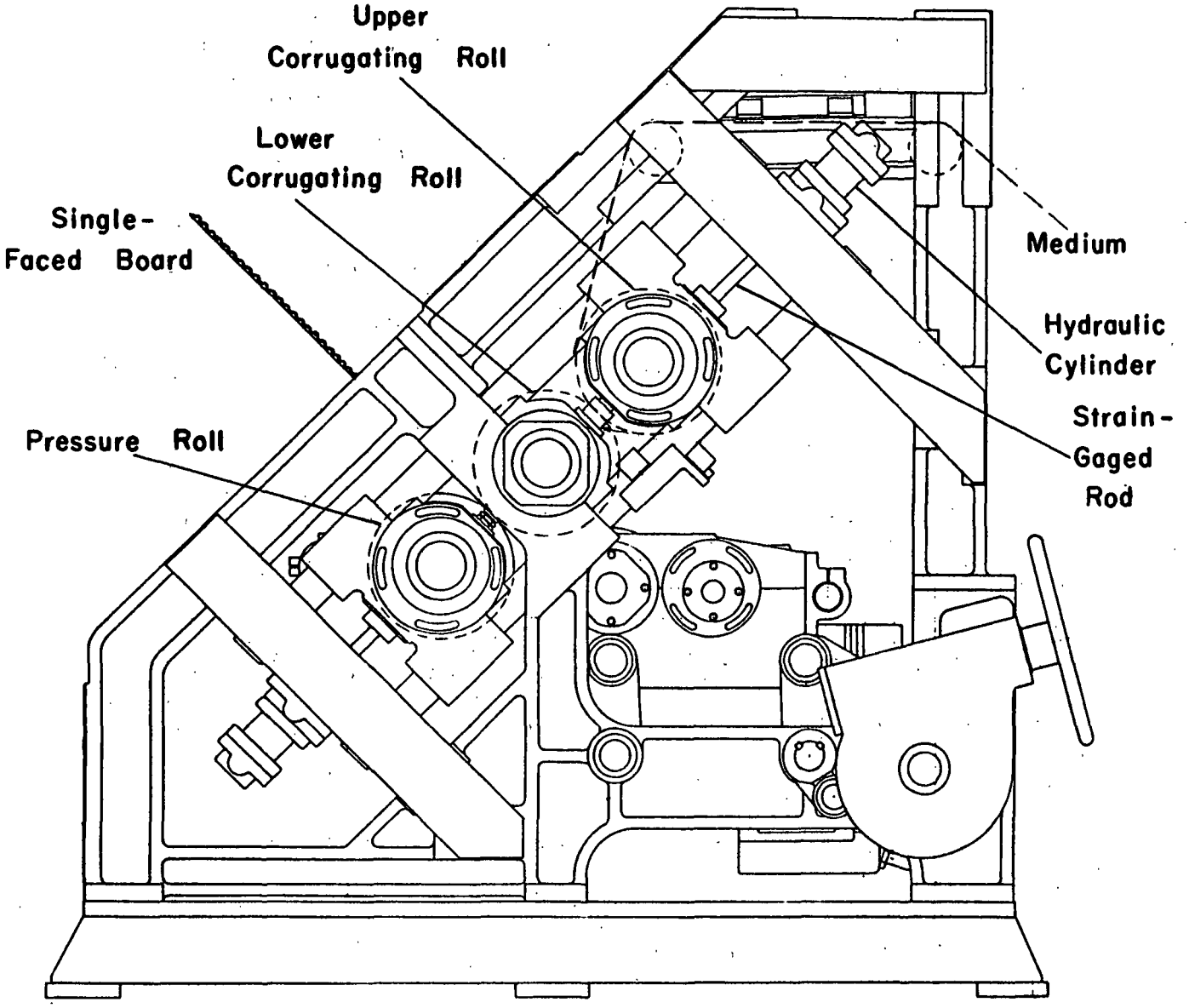

ELEVATION - OPERATING SIDE

Figure 1. Configuration of the Institute Experimental Corrugator

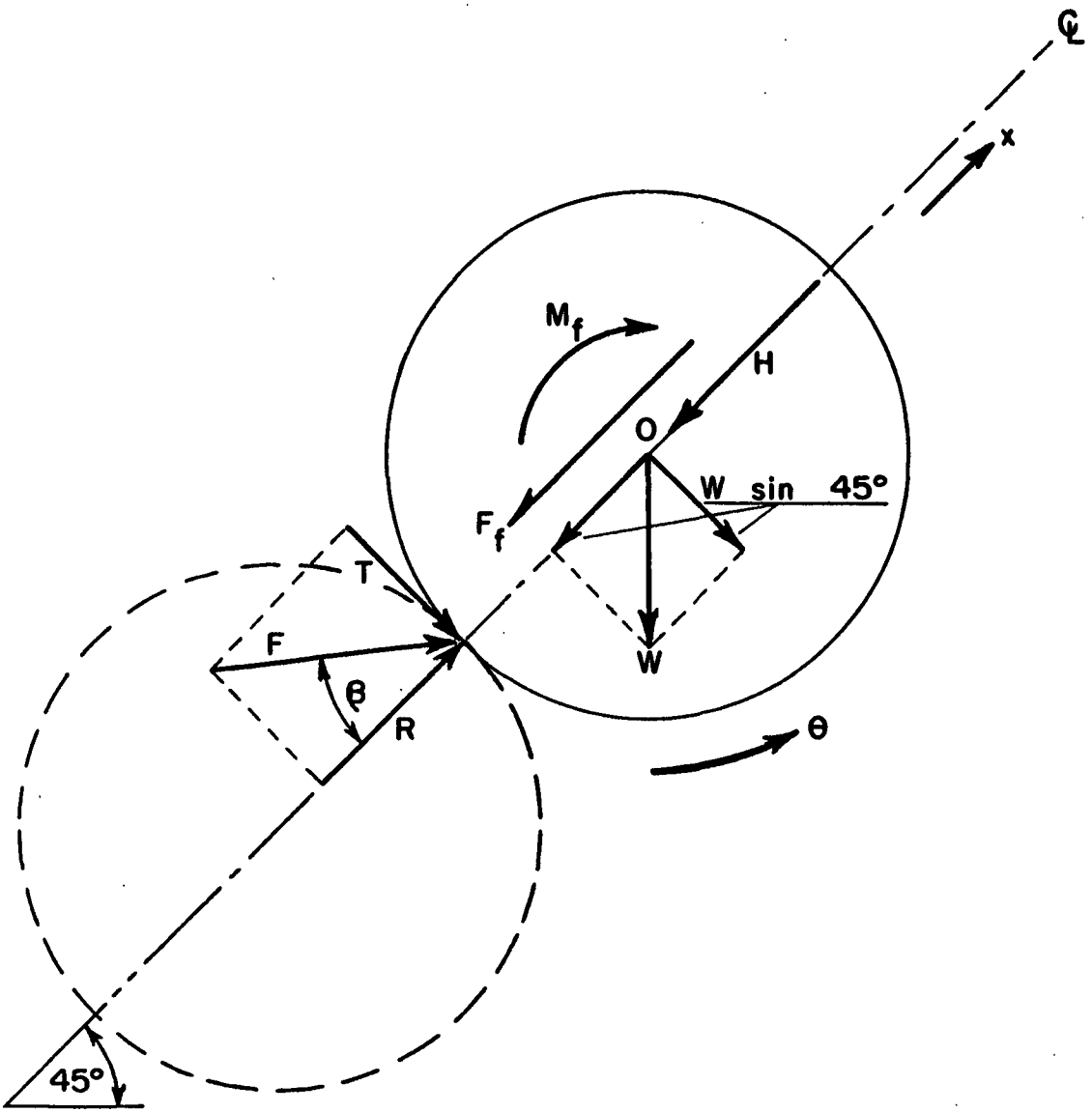

Figure 2. Forces Acting on the Upper Roll of the Institute Corrugator

in the following theoretical discussion of the molding force and the dynamics of the upper corrugating roll.

TRANSLATIONAL MOTION OF THE UPPER CORRUGATING ROLL

The displacement of the upper roll along the centerline of Fig. 2 is denoted by the co-ordinate x, taken as positive when the roll has moved upward relative to its median position. In addition to the component force R, other forces acting on the upper roll which are associated with its translational motion are gravity, sliding friction of the bearing assemblies and hydraulic loading.

The weight of the upper roll assembly, W, acts downward through the center of gravity of the assembly; the weight is estimated to be about 800 lb. The component of the weight acting parallel to the direction of roll displacement is $W \sin 45° = 800(\sqrt{2}/2) = 560$ lb. The component of weight perpendicular to the direction of roll motion (also $W \sin 45°$) is reacted by the chromed-steel guide rods on which the upper roll assembly slides. Accordingly, a force due to friction, F_f, acts in a direction opposite to the direction of roll motion. Assuming a coefficient of sliding friction, μ, independent of velocity and having magmitude 0.1, the total force of friction is $F_f = \mu W \sin 45° = (0.1)\ (560\ \text{lb.}) = 56$ lb.

The upper roll is loaded by means of a hydraulic pressure system which exerts a total force, H, along the line of roll motion. The nature of this force will be discussed in greater detail later.

From the law of motion (force = mass x acceleration), the equation of linear motion of the upper roll is

$$m\ddot{x} = R - H - F_f - W \sin 45^\circ \qquad (1)$$

when the roll is moving upward (i.e., when $\dot{x}$ is positive). In this equation $\ddot{x} = d^2x/dt^2$ = acceleration, $\dot{x} = dx/dt$ = velocity, and $m = W/g$ = mass = weight/acceleration of gravity. The forces in Equation (1) are considered as positive when directed as diagrammed in Fig. 2. (A complete list of symbols appears in Appendix A to this report.)

When the upper roll moves downward along the center line ($\dot{x}$ negative) the force of friction is directed opposite to that shown in Fig. 2, whereupon the equation of motion is

$$m\ddot{x} = R - H + F_f - W \sin 45^\circ. \qquad (2)$$

As a first approximation it will be assumed that the friction force, F_f, is independent of displacement and velocity of the upper roll. In view of the small mean value of this force (56 lb.) relative to the x-component of the weight of the roll assembly (560 lb.), it appears that any reasonable variation with time in the friction force will be inconsequential to the motion of the upper roll.

The hydraulic force, H, on the other hand, is not a constant force. Experiments have shown that it varies about its mean value of 3500 lb. (corresponding to 250 p.s.i.g. in the hydraulic lines) by about 500 lb. for each one-thousandth inch of roll displacement. This variation in hydraulic force is apparently in the nature of a mechanical spring and may be attributed to inertia of the hydraulic fluid, expansion of the hydraulic

lines and the cushioning action of nitrogen gas-filled cylinders which act as shock absorbers for the hydraulic system.

In view of the springlike characteristic of the hydraulic force, it is convenient to consider $\underline{H}$ as made up of two additive (scalar) components, namely, a statical component $\underline{H_s}$ equal to the mean value of the hydraulic force (typically 3500 lb.) and a dynamic component $\underline{H_d}$ having the characteristics of a spring. Symbolically,

$$H = H_s + H_d = H_s + k_h x \qquad (3)$$

where $\underline{H}$ = total hydraulic force, lb.

$\underline{H_s}$ = static component of hydraulic force, lb.

$\underline{H_d}$ = dynamic component of hydraulic force, lb.

$\underline{k_h}$ = spring constant of hydraulic system, lb./in.

The mean hydraulic force, $\underline{H_s}$, will be considered as acting when the upper roll is at its median displacement ($\underline{x} = 0$). This is only approximately correct inasmuch as the mean hydraulic force is really a time-average rather than a median value. It is believed that the error of this approximation is not prohibitive. In view of Equation (3), it is seen that the total hydraulic force, $\underline{H}$, varies about its mean value, $\underline{H_s}$, depending on whether the displacement, $\underline{x}$, is positive or negative.

The force, $\underline{R}$, exerted by the lower roll also may be considered as being composed of statical and dynamic scalar components, viz.,

$$R = R_s + R_d \qquad (4)$$

where $\underline{R_s}$ = static component of force exerted by lower roll, lb.

$\underline{R_d}$ = dynamic component of force exerted by lower roll, lb.

The static component, $\underline{R_s}$, is the force exerted by the lower roll when the corrugator is hydraulically loaded to its mean value, $\underline{H_s}$, but the corrugator is not running.

Substituting Equations (3) and (4) into Equation (1), the equation for upward motion of the upper roll becomes

$$m\ddot{x} = R_s + R_d - H_s - k_h x - F_f - W \sin 45°. \quad (5)$$

But under static conditions (i.e., rolls hydraulically loaded but corrugator not running)

$$R_s - H_s - W \sin 45° = 0,$$

whereupon the equation for upward motion becomes

$$m\ddot{x} = R_d - k_h x - F_f \text{ (when } \dot{x} \text{ is positive)}. \quad (6)$$

Similarly, the equation for downward motion becomes

$$m\ddot{x} = R_d - k_h x + F_f \text{ (when } \dot{x} \text{ is negative)}. \quad (7)$$

Equations (6) and (7) may be recognized as the equations of motion of a simple spring-mass system with Coulomb damping (5) subjected to a driving force, $\underline{R_d}$, and the system may be diagrammed schematically as shown in Fig. 3.

The driving force, $\underline{R_d}$, exerted by the bottom roll (and acting transversely through the corrugating medium) is given by

$$R_d = m\ddot{x} + k_h x + F_f \quad \text{(when } \dot{x} \text{ is positive)} \quad (8)$$

and

$$R_d = m\ddot{x} + k_h x - F_f \quad \text{(when } \dot{x} \text{ is negative)}. \quad (9)$$

Thus, the dynamic driving force, $\underline{R_d}$, may be calculated from numerical data on the acceleration and displacement of the upper corrugating roll, provided the "machine constants" are known, namely, mass ($\underline{m} = \underline{W/g}$), hydraulic spring constant($\underline{k_h}$) and friction force ($\underline{F_f} = \mu \underline{W} \sin 45°$). The dynamic driving force, $\underline{R_d}$, may be added to the static component, $\underline{R_s} = \underline{H_s} + \underline{W} \sin 45°$,

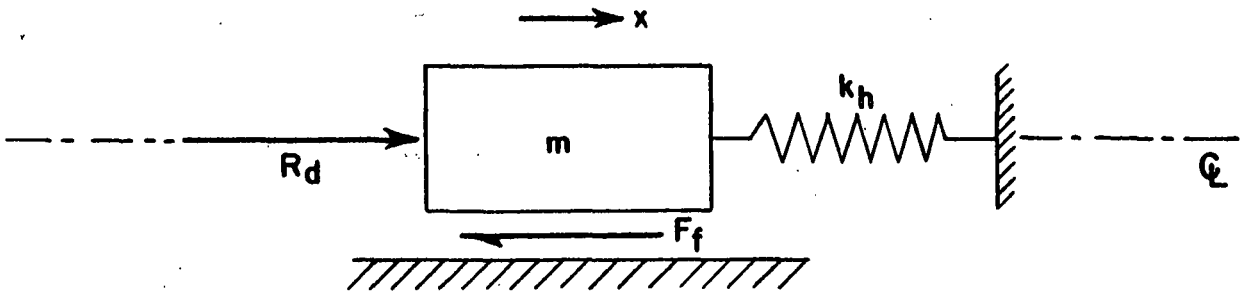

Figure 3. Spring-mass System Equivalent to Upper Corrugating Roll

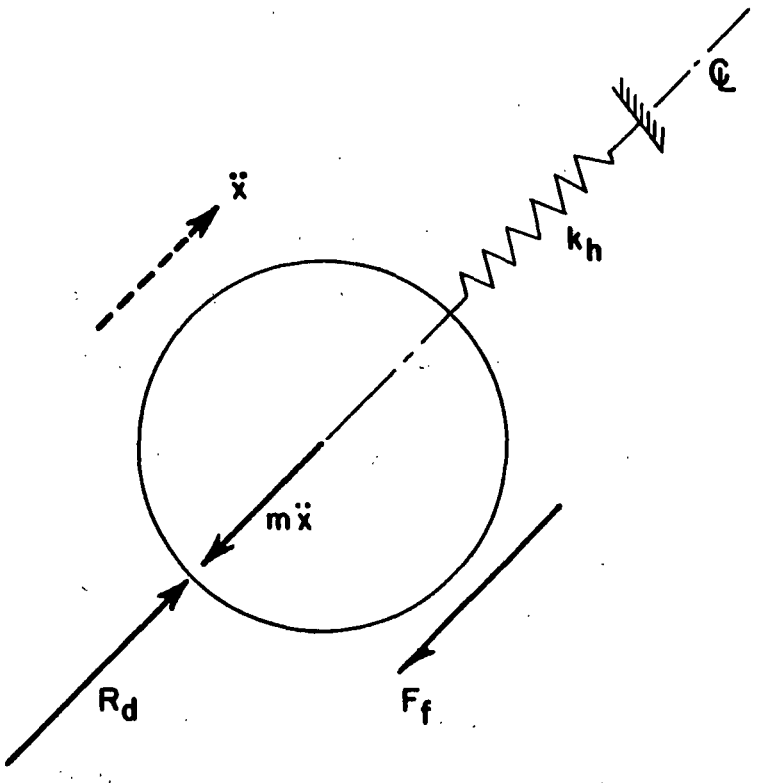

Figure 4. Dynamical System of Forces on Upper Roll in Terms of Inertial Force

corresponding to a particular hydraulic loading, to give the total force, R, exerted through the medium parallel to the line joining the roll centers, i.e., the radial component of the molding force, F.

Following the D'Alembert method of dynamical analysis (6), an inertial force may be considered as acting on the mass (i.e., upper roll assembly), having magnitude $m\ddot{x}$ and directed oppositely to the acceleration at the instant in question, as illustrated in Fig. 4. In this scheme, the analysis may be treated by the methods of statics. The equilibrium equations are

$$R_d - m\ddot{x} - k_h x - F_f = 0 \quad \text{(when } \dot{x} \text{ is positive)} \tag{10}$$

and

$$R_d - m\ddot{x} - k_h x + F_f = 0 \text{ (when } \dot{x} \text{ is negative).} \tag{11}$$

For example, when the upper roll is moving upward at a location $x = +b$ above its median displacement, but is slowing down ($\ddot{x} = -a$, i.e., negative acceleration), Equation (10) becomes

$$R_d + m\,a = k_h\,b + F_f \tag{12}$$

i.e.,

$$\left[\begin{array}{c}\text{Dynamic}\\ \text{Driving}\\ \text{Force}\end{array}\right] + \left[\begin{array}{c}\text{Inertial}\\ \text{Force}\end{array}\right] = \left[\begin{array}{c}\text{Hydraulic}\\ \text{Spring}\\ \text{Force}\end{array}\right] + \left[\begin{array}{c}\text{Friction}\\ \text{Force}\end{array}\right]$$

It is seen that at this instant two forces are effective in slowing down the roll motion, namely, the hydraulic spring force and the friction force. They are opposed by the dynamic driving force of the lower roll and the inertia of the upper roll assembly. It may be recognized that if the acceleration, a, is very large, such as occurs at the extreme point of positive displacement,

the dynamical component, R_d, of the lower roll force may have to be negative in order that Equation (12) be satisfied. This means that the total radial force, R, exerted by the lower roll must be less than its mean value, R_s, in order that the upper roll assembly be slowed down to zero velocity in its upward motion and thereafter reverse its direction.

Similarly, it may be reasoned that an increase in the total radial driving force may be required at the point of minimum roll displacement (i.e., corrugating rolls closest together) in order to give the upper roll the positive acceleration needed to reverse the direction of roll motion.

It should be noted that the dynamic components of the driving force and hydraulic force (R_d and $k_h x$) can be either positive or negative. The total radial driving force (R) and the total hydraulic force (H), however, can be only compression forces, that is, positive forces by the sign conventions adopted in this analysis.

ROTARY MOTION OF UPPER CORRUGATING ROLL

The equation of rotary motion (moment of force = moment of inertia x angular acceleration) of the upper roll is (see Fig. 2):

$$I \ddot{\theta} = Tr - M_f \qquad (13)$$

where I = moment of inertia of upper roll about its axis of rotation, lb. in. sec.^{2}

$\ddot{\theta}$ = angular acceleration of upper roll, rad./sec.^{2}

T = tangential component of molding force F, lb.

r = mean radius of upper roll, in.

M_f = moment of friction force between roll journal and bearings, lb.-in.

This equation expresses the fact that the angular acceleration of the upper roll is supplied by the tangential driving force, T, and opposed by the bearing friction, M_f.

Inasmuch as the point of driving contact between a corrugation of the bottom roll and a corrugation of the upper roll continually changes during the formation of a flute, there is no single value of the moment arm of the tangential driving force, T. It would appear, however, that the mean radius, r, of the upper roll would be a reasonable approximation to the instantaneous moment arm; for a twelve-inch diameter A-flute roll, the error in the moment arm would be no greater than 0.1 inch in six inches, that is, less than 2%.

The moment of bearing friction, M_f, in the Institute corrugator has been evaluated experimentally at ordinary operating temperatures but at very low speeds of rotation. This measurement was accomplished by wrapping a flexible tape around the upper roll when the latter was disengaged from the lower roll. A spring scale attached to the free end of the tape indicated the force necessary to overcome bearing friction while the roll was rotated at slow, uniform speed by pulling the spring scale and tape. The measured force was 30 lb., whereupon the moment of bearing friction is approximately (30 lb.)(6 in.) = 180 lb.-in. It may be anticipated that the moment of friction at practical corrugating speeds will differ by some small amount from this experimental value because of the well-recognized but generally uncertain relationship between the coefficient of friction and speed in roller bearings.

If the angular acceleration, $\ddot{\theta}$, is measured or estimated for particular operating conditions of the corrugator, the tangential driving force, T, may be calculated from Equation (13). It may be recognized that the angular acceleration of the roll may be of two types: (a) changes in nominal corrugating speed, and (b) nonsteady rotation during the period of formation of a flute. As an example of the first type of angular acceleration, suppose that the corrugating speed is increased from zero to 500 ft./min. in ten seconds. The final speed corresponds to an angular velocity of about 17 radian/second for a 12-inch diameter corrugating roll. The average angular acceleration over the ten-second period, therefore, is 1.7 rad./sec.^{2} The driving force T required to bring the corrugator up to this operating speed is given by Equation (13), namely,

$$T = (I/r)\ddot{\theta} + M_f/r. \qquad (14)$$

If the corrugator speed is maintained thereafter at 500 ft./min. (or any other constant speed), the nominal angular acceleration $\ddot{\theta}$ is zero and the driving force is reduced to

$$T = M_f/r, \qquad (15)$$

that is, a force just sufficient to overcome bearing friction. For the machine and operating characteristics cited above for the Institute corrugator, the steady-state driving force is

$$T = (180/6) = 30 \text{ lb.}$$

If the corrugator is slowed down (negative acceleration) the tangential force, T, will diminish (algebraically) from its steady-state value and may reverse direction for sufficiently large decelerations. The latter corresponds

to a braking action by the lower roll, whereupon the points of driving contact change to the opposite sides of the roll corrugations.

Regarding the second type of angular acceleration, it is believed that the conjugate tooth action of the roll corrugations is such that the roll does not turn with absolutely uniform speed during the formation of a flute, but rather is an uneven motion because of the corrugation profile and the presence of a deformable medium between the corrugations. Thus, even though the corrugator may be running at a nominally constant speed of, say, 500 ft./min., the upper roll may be momentarily speeded up and slowed down as two mating corrugations roll past each other at the center of the labyrinth. Thus, over the short time interval of 1/300 second (corresponding to the molding of an A-flute at 500 ft./min.) the upper roll may be subjected to momentary accelerations and decelerations. The driving force, $\underline{T}$, must change accordingly [see Equation (14)].

Closely allied with momentary accelerations due to tooth profile and interposition of the medium are other angular accelerations due to non-uniform velocity of the bottom (driving) roll. No drive system is perfectly uniform and it may be expected, therefore, that the motor and gear train of the lower roll induce spurious accelerations to the lower roll which are transmitted to the upper roll.

These momentary accelerations, of course, differ only in degree from the intentional angular acceleration of the upper roll as the corrugating speed is changed. If the momentary accelerations can be measured or estimated, the associated driving force can be evaluated from Equation (14).

[It should be remarked that a more exact analysis of the forces acting on the upper corrugating roll would admit the possibility that the point of application of the resultant molding force, F, (see Fig. 2) may not be precisely at the center point of the labyrinth. The force F is the resultant of a complex distribution of forces extending over a number of teeth in the labyrinth and represents the totality of all effects which may be described individually as (a) driving the upper roll, (b) forming the flutes, and (c) molding the flutes. Because of the various magnitudes and the dispersed nature of this complex system of forces, it must be admitted that the line of action of its resultant indeed may intersect the periphery of the upper roll at a point other than on the line of roll centers.

The effect of this refinement in the analysis is that the line of action of the component force, R, parallel to the line of roll centers, does not pass through the center of the upper roll, but rather is eccentric by some amount, e. Accordingly, the equation of angular motion, Equation (13), would be amended by adding a term, R e, to the right-hand side, accounting for the moment of force R about the center of the upper roll. The equations for linear motion of the upper roll would remain unaffected.]

DETERMINATION OF TOTAL MOLDING FORCE, F

The resultant molding force, F, is given in terms of its vector components, R and T, by

$$F = \sqrt{R^2 + T^2} \tag{16}$$

and its line of action is inclined to the line of roll centers by the angle

$$\beta = \arctan (T/R). \tag{17}$$

It is evident from the foregoing theoretical discussion that the major undetermined quantities required for estimation of molding force are (a) the linear acceleration of the upper roll parallel to the line of roll centers, and (b) the momentary angular acceleration while the upper roll is driven at a nominally constant corrugating speed. On the assumption that the linear acceleration has the dominant effect on molding force, it was decided to pursue the investigation of the unknown accelerations in the order listed above. The remainder of this report, therefore, is concerned with a preliminary study of the linear accelerations associated with jumping of the upper roll.

EXPERIMENTAL PROGRAM

The experimental program consisted essentially of determining the linear displacement and acceleration of the upper roll (A-flute) and the hydraulic spring force, $\underline{k_h x}$, at various corrugating speeds for a given medium, so that the driving force, $\underline{R_d}$, acting transversely through the medium at the center point of the labyrinth could be calculated from Equations (8) or (9) [or, alternatively, Equations (10) and (11)].

Displacement of the upper roll was measured by means of a displacement transducer which has been developed for allied studies concerning the clearance between the upper and lower rolls during corrugating (4). As illustrated in Fig. 5, the displacement transducer measures the motion of the upper roll relative to the lower roll by means of a strain-gaged ring compressed between two pivoted arms which ride on the shoulders of the corrugating rolls. The measurement was displayed as a curve of displacement versus time on the screen of a dual-beam oscilloscope and recorded on film by means of a Polaroid camera attachment. The displacement transducer was calibrated by means of a machinist's micrometer, giving a calibration factor of 0.00016 inch of roll displacement per centimeter graduation on the oscilloscope screen.

The instantaneous hydraulic force, $\underline{k_h x}$, was measured by means of a strain-gaged, one-inch diameter rod which connects the hydraulic piston and the bearing assembly at that end of the upper corrugating roll whose motion was measured with the displacement transducer (see Fig. 1). Four 500-ohm, SR-4 strain gages, cemented longitudinally and circumferentially on the rod, constituted the arms of a Wheatstone bridge, on which 18 D.C. volts were impressed.

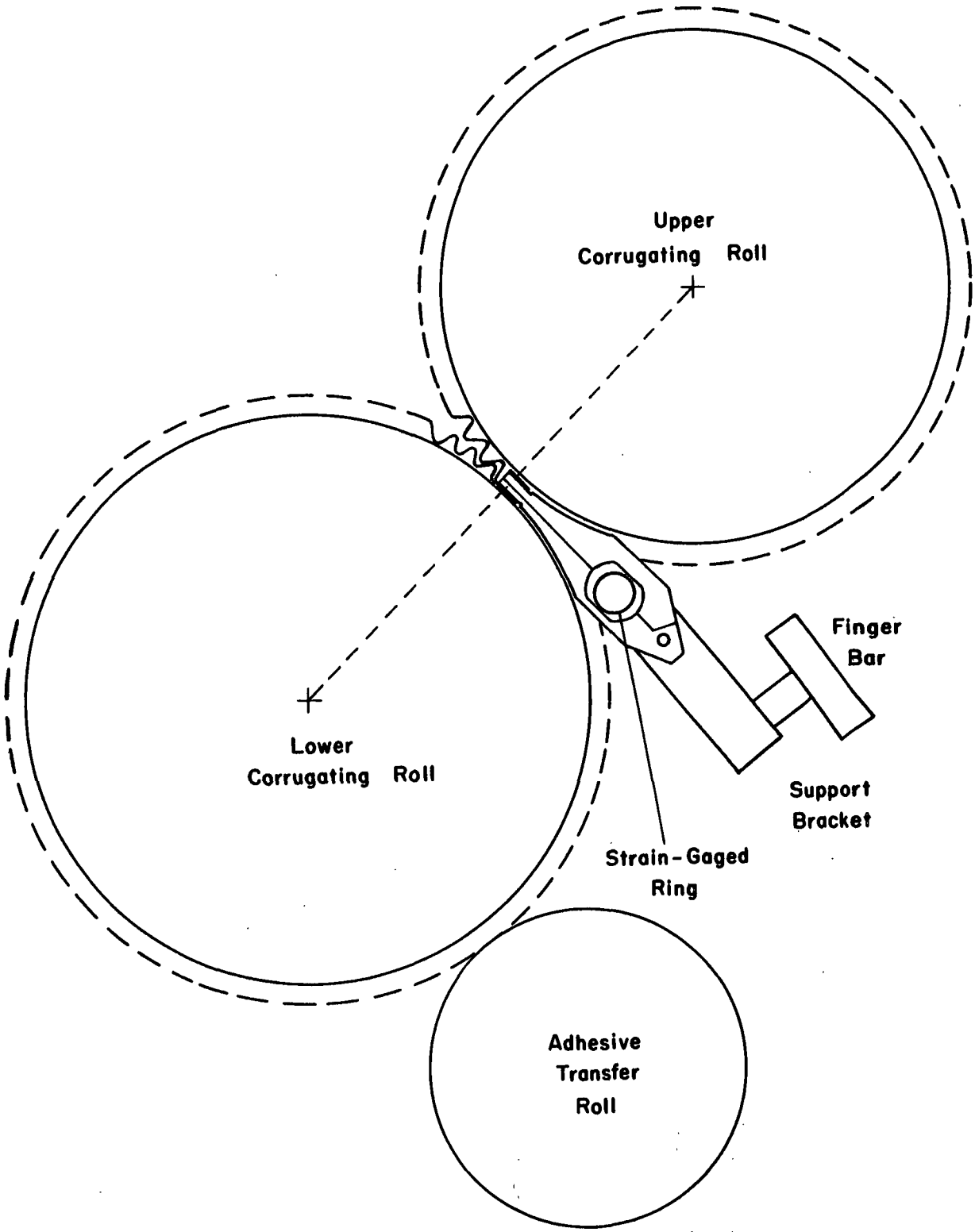

Figure 5. Displacement Transducer Employed for Measurement of Roll Motion

The gages were arranged in the bridge so that bending strains cancelled and only the axial strain in the rod was measured. The bridge was balanced to zero output with the corrugator stopped, whereupon the output of the bridge during corrugating was proportional to the dynamic component, $k_h x$, of the hydraulic force at one end of the upper corrugating roll. The bridge output was displayed as a curve of force versus time by the second beam of the dual-beam oscilloscope and photographed along with the aforementioned displacement versus time trace.

The strain gage bridge on the rod was calibrated statically by manually adjusting the hydraulic pump valve to give ± 30 p.s.i.g. about the mean pressure of 250 p.s.i.g. and observing the displacement of the oscilloscope trace. At maximum sensitivity of the oscilloscope the calibration factor was 5.3 p.s.i. per centimeter on the oscilloscope. Inasmuch as the hydraulic piston area is seven square inches, the calibration factor may also be expressed as 37.1 lb. per centimeter. This calibration was checked satisfactorily later on a universal testing machine. Because Equations (8) and (9) involve all forces acting on the upper corrugating roll, it was assumed that the second hydraulic cylinder at the other end of the roll acted at the same instantaneous pressure as the measured end, whereupon the calibration factor for the total (dynamic) hydraulic force is 74.2 lb. per centimeter on the oscilloscope screen.

The calibration of the strain-gaged rod described above suffers from two shortcomings which should be improved upon in future work. First, in this preliminary study, the calibration was performed at only one level of hydraulic pressure above and below the mean pressure, namely, at ± 30 p.s.i.g., corresponding to ± 420 lb. hydraulic force. This mode of calibration does not determine

the linearity of the transducer at intermediate and more extreme levels of pressure. It will be seen from the data presented later in this report, however, that the measured values of hydraulic force were within the calibration range, so that interpolation, rather than extrapolation, of the calibration was performed.

Secondly, and perhaps of greater significance, is that the calibration was performed statically whereas the measurements during corrugating were highly dynamic. It is believed that the static calibration led to underestimation of the dynamic hydraulic force, for the following reason. Most ductile materials such as steel exhibit an increased modulus of elasticity with increase in the rate of load application. That is, relative to a slowly applied load, a rapidly stressed body will undergo less strain. Equivalently, a greater dynamic stress is required to give the same strain as was obtained with the stress levels employed in the static calibration of the strain-gaged rods. A dynamic strain signal obtained during corrugating, therefore, is actually caused by a higher load than would be inferred from the results of a static calibration.

Figure 6 is a typical photograph of oscilloscope curves of displacement and hydraulic force as a function of time. This photograph was taken while corrugating a 26-lb. semichemical medium at 100 f.p.m. with A-flute rolls. Time increases from right to left; the distance between successive grid lines corresponds to 2 milliseconds (i.e., 0.002 second). The lower curve is roll displacement with positive $\underline{x}$ measured upward (one grid division = 0.16×10^{-3} inch) and the upper curve is hydraulic force, $\underline{k_h x}$, with compression increasing in the upward direction (one grid division = 74.2 lb., accounting for both ends of the roll).

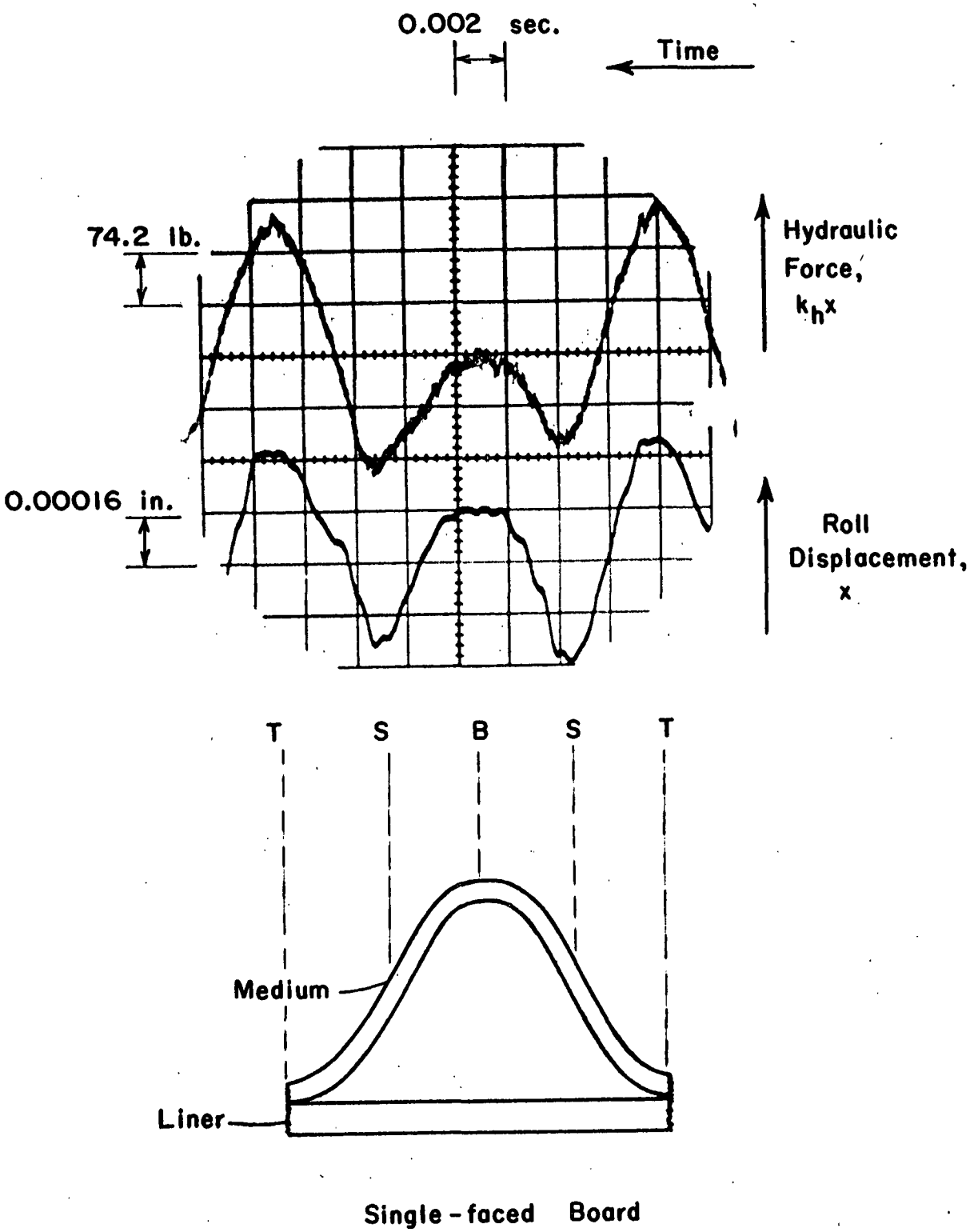

Figure 6. Typical Oscilloscopic Record of Dynamic Hydraulic Force and Roll Displacement (26-lb. Semichemical Medium Corrugated at 100 f.p.m. with A-flute Rolls)

Past experience (4) identifies the lower peaks, points S, of the curves as the instant when the side walls of a corrugator roll tooth are at the center point of the labyrinth. The lesser of the three maxima, point B, of each curve corresponds to a root of the bottom roll at the center point (the medium in this root is the unadhered arch of the flute in single-faced board); the greater of the three maxima, points T, are roots of the upper roll (corresponding to the adhered arches of a flute in single-faced board). Thus, one flute corresponds to the curve starting from one point T and ending at the following point T.

It may be noted that the maxima and minima of the force and displacement curves coincide timewise and, in general, the two curves are substantially parallel throughout. That is, as the upper roll moves away from the lower roll (increasing x) the hydraulic pressure increases proportionately, as would be anticipated, and, conversely, as the roll displacement diminishes, the hydraulic pressure also decreases. For the medium and operating conditions of Fig. 6, the maximum roll displacement was about six ten-thousandths of an inch and the hydraulic force changed by about 375 lb. At a maximum point on the curves the increased hydraulic pressure provides the negative acceleration required to bring the roll velocity to zero and reverse its direction. At a minimum point, the hydraulic pressure reaches its least value which, in conjunction with the driving force supplied by the lower corrugating roll, accounts for the large positive acceleration necessary to reverse the roll motion.

A graphical differentiation of the displacement curve at any instant of time provides an estimation of the acceleration, $\ddot{x}$, of the upper roll and

thereby enables calculation of the lower roll driving force, R_d, at that instant [Equations (8) or (9)]. The determination of acceleration was accomplished as illustrated in Fig. 7. The accelerations of greatest interest are those at the peaks of the displacement curve (e.g., point T) since they are the maximum accelerations and are associated with the maximum forces acting on the upper roll. It is impossible, however, to determine an instantaneous acceleration graphically from a displacement vs. time curve; the best that can be done is to determine the average acceleration over a finite time interval, Δt (e.g., from A to T) and then repeat the process for successively smaller intervals of time, thereby approaching the instantaneous acceleration at T in the limit. On the other hand, the repetitive process is hardly warranted for a first approximation. It may be shown (see Appendix B) that with harmonic motion ($x = \sin t$), an interval Δt as great as one-half of the quarter-period of the motion (e.g., approximately points A to T in Fig. 7) will lead to an error of only -10% in the calculation of the instantaneous acceleration at point T.

To estimate the acceleration at point T, therefore, a point A was located where the displacement curve visibly departed from linearity (i.e., where the velocity was not constant). A tangent line was drawn to the curve at A. Inasmuch as the slope of the tangent line is proportional to the velocity, $\dot{x}_1$, at A, this velocity was readily calculated in units of inches/second. The velocity, $\dot{x}_2$, at the apex of the curve, point T, is zero since the slope of the tangent line is zero at this point. Then the average acceleration, $\bar{\ddot{x}}$, over the time interval, Δt, is given by

$$\bar{\ddot{x}} = \frac{\dot{x}_2 - \dot{x}_1}{\Delta t} = \frac{-\dot{x}_1}{\Delta t}$$

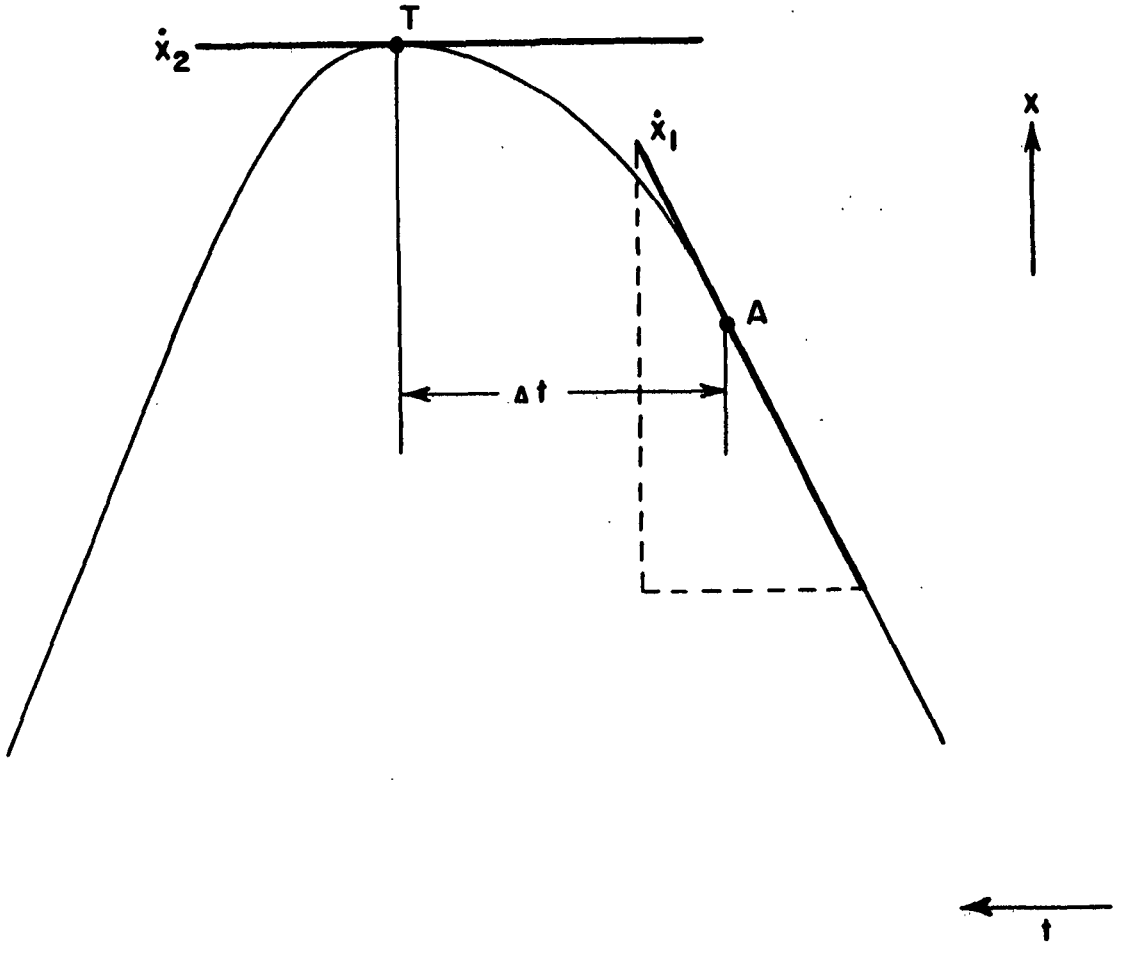

Figure 7. Illustration of a Graphical Method of Computing Acceleration from a Displacement vs. Time Curve

Inasmuch as the hydraulic force, $\underline{k_h x}$, may be read from the force-time curve, Equation (8) may be used to calculate the lower roll force, $\underline{R_d}$, acting at the instant of time corresponding to point T.

It may be appreciated that, due to the low magnification of the displacement curves shown in Fig. 6, considerable error may be introduced in the estimation of acceleration when fitting a tangent line to the curve. In an effort to minimize this type of error, additional photographs were obtained (at a given corrugating speed) with a magnified time scale (i.e., faster sweep of the oscilloscope beam). In this way an enlarged trace of each typical maximum and minimum point of the displacement curve was made available for acceleration measurements. In some instances the oscilloscope sweep was synchronized with the event so that successive peaks of the same type appeared superimposed on the photograph. Figure 8 is a photograph of three successive peaks of type T (c.f., Fig. 6) taken at a sweep speed of 0.4 millisecond per centimeter. The superposition of peaks in Fig. 8 permits construction of an average slope when calculating $\underline{\dot{x}_1}$, thereby alleviating somewhat the problem of small sampling which would otherwise accompany increased sweep speeds.

Am undesirable consequence of working with photographs with increased sweep speeds, such as Fig. 8, was the loss of a reference level for reading displacement, $\underline{x}$, or hydraulic force, $\underline{k_h x}$, inasmuch as the adjacent peaks of type S and B of Fig. 6 do not appear in Fig. 8. Thus, while a photograph such as Fig. 8 yielded an improved estimate of acceleration of each characteristic peak, the corresponding values of $\underline{x}$ or $\underline{k_h x}$ required for

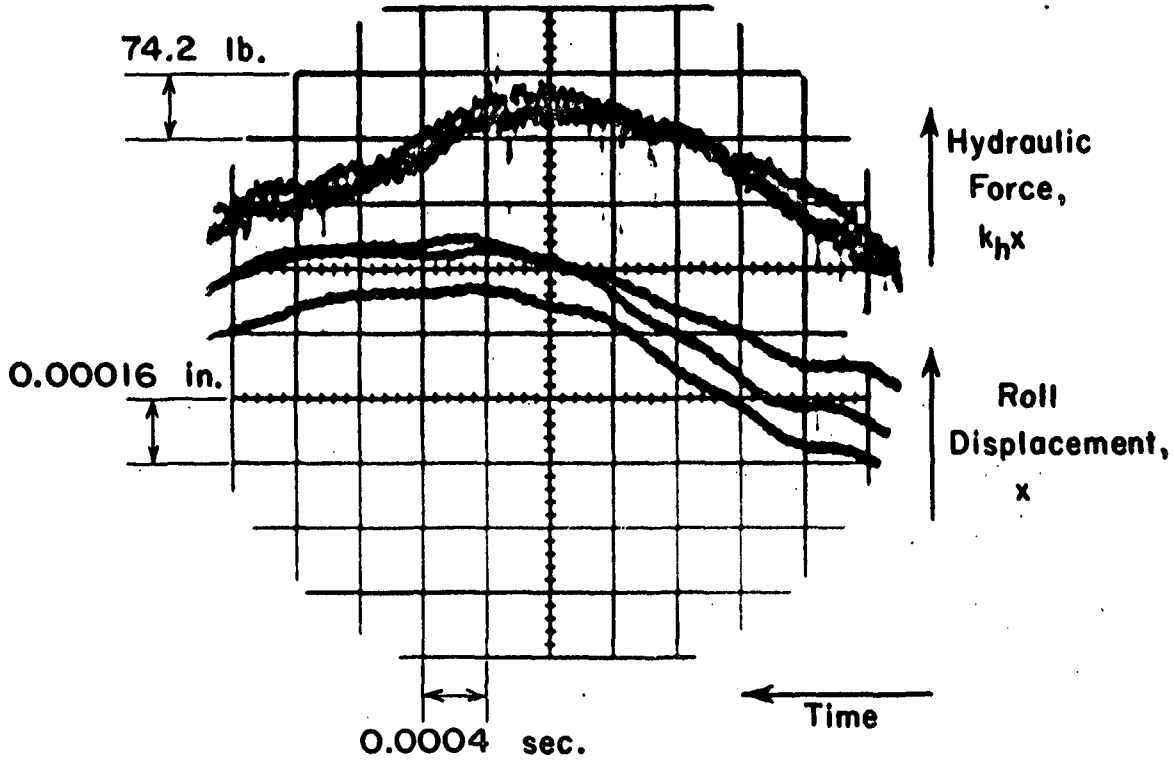

Figure 8. Oscilloscopic Record of One Type of Peak on Displacement and Hydraulic Force Curves, Obtained with Fast Sweep (26-lb. Semichemical Medium Corrugated at 100 f.p.m. with A-flute Rolls)

evaluation of Equations (8) or (9) were unknown. The only recourse was to read $\underline{k_h x}$ from photographs such as Fig. 6 and read $\underline{\ddot{x}}$ from photographs such as Fig. 8, recognizing that different corrugator teeth undoubtedly were involved in the two photographs and, therefore, an unavoidable sampling error may have been incurred.

It should be remarked that a better experimental technique would be to substitute an accelerometer for the displacement transducer. An accelerometer is a transducer which measures acceleration, $\underline{\ddot{x}}$, directly and can display it on the oscilloscope screen as a function of time. Thus, one photograph, encompassing numerous consecutive flutes, would yield $\underline{\ddot{x}}$ and $\underline{k_h x}$, whereupon the driving force of the lower roll could be calculated with much less labor and presumably greater accuracy.

Using the procedure described in the preceding paragraphs, oscilloscopic records were obtained of the corrugating of a 26-lb. semichemical medium at corrugating speeds of 40, 100, and 300 f.p.m. One additional set of photographs was taken at a corrugating speed of 40 f.p.m. with no medium, that is, bare corrugating rolls.

DISCUSSION OF RESULTS

Oscilloscopic records of the linear motion of the upper corrugating roll and the hydraulic force by which the upper roll was loaded were obtained while corrugating a 26-lb. semichemical medium at 40, 100, and 300 ft./min. with A-flute rolls and without the medium at 40 ft./min. The peak accelerations of the upper roll were estimated from its displacement vs. time curves. The above-mentioned measurements enabled calculation of the radial driving force exerted on the upper corrugating roll by the lower roll (i.e., the component of the driving force which acts parallel to the line joining the centers of the rolls). Inasmuch as this force acts transversely through the corrugating medium at the center point of the labyrinth, it is involved in the molding process of corrugating. Variations in the driving force may be expected to lead to varying degrees of flute molding and possibly may be related therefore to (a) the occurrence of highs and lows and leaning flutes in the corrugated boards and (b) runnability.

Table I contains the significant experimental data and major results of the calculation from this exploratory study of the effect of corrugating speed with and without a medium. For example, at a corrugating speed of 40 ft./min. without medium, graphical determinations were made (from three curves) of the peak acceleration when the root of the top roll was at the center point of the labyrinth. The three determinations of acceleration ranged from -37 to -80 in./sec.^{2} with a mean value of -65 in./sec.^{2} The negative sign prefixing these accelerations means that the upper roll was slowing down in its upward motion (sometimes termed

TABLE I

EXPERIMENTAL DATA AND CALCULATED DRIVING FORCE AT VARIOUS CORRUGATING SPEEDS

Corrugating Speed, ft./min.	Medium	Location on Corrugator Tooth Profile	Number of Curves in Acceleration Estimate	Acceleration, $\ddot{x}$, in./sec.^{2} Mean	Acceleration, $\ddot{x}$, in./sec.^{2} Range	Dynamic Hydraulic Force, $k_h \ddot{x}$, lb.	Driving Force of Lower Roll, lb. Dynamic, R_d	Driving Force of Lower Roll, lb. Total,[c] R
40	None	Root of top roll	3	-65	-37 to -80	+400	+320	+4380
		Root of bottom roll	3	-50	[a]	+150	+100	+4160
		Side wall	8	+785[b]	+720 to +850	-400	+1175	+5235
40	26-lb. semichem.	Root of top roll	4	-22	[a]	+195	+205	+4265
		Root of bottom roll	3	-16	[a]	+ 95	+115	+4175
		Side wall	3	+115	[a]	-195	-10	+4050
100	26-lb. semichem.	Root of top roll	5	-180[b]	-160 to -200	+170	-150	+3910
		Root of bottom roll	6	-78	[a]	+115	+10	+4070
		Side wall	6	+190[b]	+180 to +200	-170	+170	+4230
300	26-lb. semichem.	Root of top roll	3	-1430	-870 to -2150	+130	-2785	+1275

[a] Acceleration is graphical average of several curves; hence range not calculated.
[b] Mean of two graphical averages.
[c] Static component, R_s = +4060 lb., corresponding to 250 p.s.i.g. in hydraulic system.

"deceleration") and reversing its direction of motion. From supplementary oscilloscope photographs taken at the same corrugating speed, it was determined that the hydraulic compressive force, $k_h x$, on the upper roll was 400 lb. above its mean (static) value of 3500 lb. (the latter corresponding to a mean gage pressure of 250 p.s.i.). Substituting these values of acceleration and dynamic hydraulic force into the equation of roll motion, Equation (8), the dynamic driving force, R_d, of the lower roll was found to be +320 lb. Inasmuch as the static component of the lower roll force ((corresponding to corrugating speed of zero but with hydraulically loaded rolls) was 4060 lb., the instantaneous value of the lower roll force, parallel to the line of centers of the corrugating rolls, was estimated to be 4380 lb., that is, 320 lb. above its static value.

The data for the root of the bottom roll indicated that the absolute value of the acceleration was somewhat less than for the top roll root, namely, -50 vs. -65 in./sec.^{2}, as may be anticipated since the upper roll of this pair of corrugating rolls characteristically does not move as far away from the lower roll for this root. Accordingly, the driving force exerted by the lower roll was less, namely, 4160 vs. 4380 lb.

The acceleration of the roll when the side wall was at the center point (bare rolls) was an order of magnitude greater than the roll root accelerations, namely, +785 in./sec.^{2} This acceleration is positive because the upper roll has come nearest to the lower roll and is starting to move away. On the other hand, the dynamic hydraulic force has reached a minimum value for the side wall, namely, -400 lb., meaning that the total hydraulic force is 400 lb. less than mean hydraulic force, namely, 3500 lb. In spite of the

decrease in hydraulic force, the large positive acceleration required that the driving force exerted by the lower roll increase to 5235 lb. in order to reverse the direction of motion of the upper roll.

It may be of interest to note that the acceleration at the side wall when a medium was being corrugated at 40 ft./min. was only +115 in./sec.^{2}, as contrasted with +785 in./sec.^{2} for the bare rolls. Accordingly, the driving force was appreciably less when corrugating a medium, namely, 4050 vs. 5235 lb. Thus, running the corrugating rolls bare caused a substantially larger compressive force between the corrugator rolls and explains why an operator is cautious about running the rolls bare beyond, say, 50 ft./min. for fear of damaging the rolls.

The accelerations corresponding to the root of the top roll at all three corrugating speeds (40, 100 and 300 f.p.m.) with medium are seen to be -22, -180, and -1430 in./sec.^{2}, respectively. These accelerations are in the ratio of approximately 0.12:1:8, while the square of the corresponding corrugating speeds are in the ratio 0.16:1:9. If the roll motion were exactly simple harmonic, the accelerations would be in the ratio of the square of the corrugating speeds (for equal amplitudes of motion) (7). While the roll displacement curves are visibly not exactly simple harmonic, the degree of similarity between the acceleration ratios and the speed-squared ratios lends credibility to the experimental determinations of accelerations.

In examining the data of Table I, caution should be exercised when comparing the driving force at the roots vs. driving force at the side walls.

These forces should not be interpreted as stresses (that is, force per unit area). The distribution of these forces along the tooth profile (that is, stress) is not known and is outside the scope of this report. Thus, the observation that the side wall force is, in two instances, greater than the force at the root does not necessarily mean that the side wall stress is greater than the root stress, because different areas are probably involved. On the other hand, root forces may be compared directly in terms of stress, since approximately the same area is involved for all roots. Furthermore, variations in the driving force at a given root should be meaningful to a study of high-lows, leaning flutes and stress relief inasmuch as the forces should be in approximately the same ratio as the (unknown) stresses.

When corrugating a medium, there appears to be a trend to lower driving force at a root with increase in corrugating speed. For example, at a root of the top roll (corresponding to the adhered arch of the flute in single-face board) the driving force was 4265, 3910, and 1275 lb. at 40, 100, and 300 ft./min., respectively. Similarly, the force at a root of the bottom roll decreased from 4175 to 4070 lb. as the speed was increased from 40 to 100 ft./min., although the difference in force in this case may not be significant. These data indicate, however, that the intensity of the radial component of the transverse molding force diminished with increase in corrugating speed. A decrease in molding force, in turn, probably would lead to less well-formed flutes in the corrugated board, which may be the cause, therefore, of more severe high-lows as corrugating speed increases (8). Furthermore, a decrease in molding force may result in less stress relief in the medium just preceding the transverse

compression zone, thereby increasing the probability of flute fracture in the late stages of flute forming. In this sense, a decrease in molding force due to increase in corrugating speed may be one of the determining factors in the runnability of a medium.

By way of a mechanical explanation for the decrease in driving force at a root as speed increases, it may be visualized in the following terms: the inertia force of the upper roll (tending to throw the roll outward at the apex of its outward movement) becomes greater with increase in speed and consequently a larger fraction of the total available hydraulic force is required to bring the roll motion to a halt (the force of friction being constant). This leaves a smaller fraction of the total hydraulic force pressing against the roll and, accordingly, the lower roll does not need to exert as great a force against the upper roll.

Viewed in another way, when the upper roll is near the apex of its outward movement, the dynamic driving force plus the inertia force must equal the dynamic hydraulic force plus the force of sliding friction, as discussed in conjunction with Equation (12). The build-up in the hydraulic force is limited by the magnitude of the outward displacement of the upper roll and apparently does not change vastly with increase in corrugating speed. The force of friction may be regarded as essentially constant. Thus, an increase in inertia force (approximately as the square of the speed) demands that the driving force at the apex of roll movement decrease with increase in corrugating speed.

On the other hand, the driving force, R, at the side wall increased from 4050 to 4230 lb. when the corrugating speed was increased from 40 to 100 f.p.m. Unfortunately, the experimentation was not extensive enough to determine whether this difference is statistically significant.

The aforementioned trends to lower molding force at the roots and higher molding force at the side wall have been partially verified by measurements of the caliper of the tips and side walls of flutes in single-faced combined board. Each of the six types of corrugating medium listed in Table II was corrugated in the Institute's single-facer at two speeds. Samples were obtained with both A- and B-flute corrugating rolls. Flutes were cut from each sample of single-faced board and calipered at the unadhered tip and at the two side walls by means of a dial indicator on a rigid frame. The diameter of the contact anvil of the indicator was 0.125-inch for A-flute samples and 0.081 for B-flute samples. The average caliper for the several samples and operating conditions are shown in Table II.

By way of general comment on the data of Table II, it may be noted that, in general, the caliper of the flute tips and side walls was less than the caliper of the medium before corrugating, as would be anticipated. The greatest reduction in caliper occurred at the tips, ranging from about 30 to 45% of the initial medium caliper in both A- and B-flute board. The reduction in caliper at the side walls never exceeded 20%. These data indicate that the molding <u>stress</u> at the side wall is less than at the flute tip, even though the molding <u>force</u> may be greater at the side wall than at the tip, as discussed in connection with the data of Table I. In a few instances, the

TABLE II

EFFECT OF CORRUGATING SPEED ON CALIPER OF TIP AND SIDE WALLS OF FLUTE

Type of Medium	Speed, f.p.m.	Medium Caliper, point: Before Corrugating	After Corrugating: Front Side Wall	Diff., % [a]	Tip	Diff., % [a]	Back Side Wall	Diff., % [a]
			A-Flute					
Straw	450	9.4	8.0	-15	6.0	-36	8.3	-12
	900	9.4	9.3	- 1	6.4	-32	8.9	-5
Northern Semichemical	450	9.5	8.1	-15	5.5	-42	8.2	-14
	750	9.5	9.1	- 4	6.1	-36	8.8	- 7
Southern Semichemical	450	10.2	8.3	-19	5.5	-46	8.7	-15
	900	10.2	9.3	- 9	5.7	-44	9.3	- 9
Southern Semichemical	450	13.1	11.2	-14	7.9	-40	11.8	-10
	875	13.1	11.8	-10	8.6	-34	11.6	-11
Bogus	450	9.7	8.3	-14	5.5	-43	8.5	-12
	600	9.7	8.6	-11	5.9	-39	8.6	-11
Kraft	450	9.1	7.9	-13	5.2	-43	8.3	- 9
	900	9.1	8.8	- 3	5.8	-36	8.5	- 7
			B-Flute					
Straw	450	9.4	9.8	+ 4	5.8	-38	9.9	+ 5
	900	9.4	8.7	- 7	6.5	-31	8.9	- 5
Northern Semichemical	450	9.8	9.0	- 8	5.8	-41	10.4	+ 6
	750	9.8	9.0	- 8	6.3	-36	9.2	- 6
Southern Semichemical	450	10.3	10.2	- 1	5.8	-44	10.6	+ 3
	750	10.3	9.8	- 5	6.2	-40	9.4	- 9
Southern Semichemical	450	13.4	11.8	-12	8.5	-37	11.1	-17
	750	13.4	11.4	-15	8.9	-34	10.8	-19
Bogus	450	10.6	9.5	-10	6.1	-42	9.8	- 8
	600	10.6	8.8	-17	6.2	-42	9.0	-15
Kraft	450	8.8	8.9	+ 1	5.5	-38	9.2	+ 4
	900	8.8	8.1	- 8	5.9	-33	8.1	- 8

[a] Based on caliper of medium before corrugating.

flute side wall caliper exceeded the medium caliper before corrugating--by as much as 5%. This discrepancy probably reflects either (a) sampling variation in the medium or (b) the fact that the technique of measuring flute side wall caliper was somewhat less accurate than the tip measurements (the gage was better suited to measurement of the arch than of the double-curved side wall element).

To the point of the present inquiry, it may be seen from the data of Table II that in all instances the residual caliper at the flute tip increased when the corrugating speed was increased. The increase in residual caliper ranged from 0.1 to 0.7 of a point. This observation agrees with the noted trend for molding force at the roots to decrease with increase in speed, because the lower the force at a root, the lower would be the molding stress; a lower stress during molding, in turn, would lead to less nonrecoverable strain in the transverse direction and hence a higher residual caliper. It should be mentioned that the flute tip which was measured corresponds to the root of the lower corrugating roll. Of the two types of roots, the lower roll root exhibited the lesser decrease in molding force with increase in speed. It may be anticipated that the adhered tips of the flutes experienced somewhat greater differences in residual caliper due to increase in corrugating speed.

The effect of speed on residual caliper of the flute side walls is less clear-cut. In the case of the B-flute samples, the side wall caliper decreased with increase in speed in all cases except one, as would have been anticipated from the noted trend of increase in molding force at higher speed. The A-flute board displayed the opposite trend, however, which is contrary to

what would be expected from the force determinations. As mentioned earlier, less confidence can be placed in the side wall caliper measurements because of the technique employed in gaging.

Taken in entirety, the measurements of medium caliper of the flutes lend credence to the trend noted in the study of upper roll motion, namely, that an increase in corrugating speed decreases the molding force at a root of the roll (i.e., flute tip) and increases the molding force at the side walls. It may also be noted that this result appears to be in agreement with the qualitative description of Peters (3) that "... at higher speeds the corrugating medium becomes crushed by the hard blows of the jumping roll and there is a rather strong trend towards 'high-low's' because the contact is missing." Moreover, the observation that the force at the side wall becomes greater at higher speed may be allied to Wilson's (2) conclusion that excessive "drop action" can cause rupture of the flute side walls.

It may be recalled that the tangential force, T, required to overcome bearing friction and thereby maintain a nominally constant corrugating speed was estimated to be 30 lb. This estimate ignored the effect due to any momentary changes in angular acceleration of the upper roll such as may arise from conjugate action of the upper and lower roll corrugations in conjunction with the medium or from the lower roll drive system. In view of the small magnitude of the tangential force, T, relative to the radial forces, R, shown in Table I, it appears that, in general, the total molding force, F, was essentially equal to the radial component and was directed nearly parallel to the line joining the roll centers. That is, from Equations (16) and (17),

$$F = \sqrt{R^2 + T^2} \doteq R$$

and

$$\beta = \arctan (T/R) \doteq 0$$

On the other hand, diminution of the radial driving force, R, with increase in corrugating speed leads to a resultant molding force which is more inclined away from the center line and the tangential driving component becomes of increasing important to the magnitude of the total molding force. The relative importance of the tangential driving force cannot be fully evaluated, however, until the significance of momentary angular acceleration is determined. The discussion of these angular accelerations which was presented in Theoretical Considerations makes evident that an experimental program closely paralleling the present study of linear accelerations is required.

Because of the preliminary nature of this investigation, the trends appearing in the data of Table I perhaps should be viewed with caution. Inasmuch as this study was primarily an exploration of the theoretical and experimental method, the data are of only limited extent. As may be noted, the data reflect a very small sampling of roll teeth--at most, eight at any one speed. Furthermore, the experimental method demanded that the dynamic hydraulic force, $\underline{k}_h \underline{x}$, be determined at a different tooth from that for which the acceleration was calculated. Hence, variations in tooth profile or medium properties could introduce error into the reported analysis.

It is believed, however, that the results of this analysis demonstrate the feasibility of this theoretical and experimental approach to determining the nature and magnitude of the transverse molding forces at the nip of the

corrugator. Moreover, it is believed that with a few modifications in the method it will be possible to study efficiently the variations in transverse molding force and thereby determine whether the variations are related to high-and-low flutes and runnability. As discussed earlier, a major improvement probably will be achieved by the substitution of an accelerometer for the present displacement transducer. This will permit direct recording of roll acceleration and hydraulic force over a substantial number of consecutive flutes, say, 20 or 25. Moreover, the corresponding single-faced board can be sampled, using a technique already developed in studies of roll clearance (4). Thereupon, the transverse molding force may be compared directly with the height and appearance of the flutes in the single-faced board. Work along these lines is in progress.

Another modification which is being incorporated in the current experimental work is the strain gaging of the connecting rod between roll and hydraulic cylinder at the opposite end of the corrugating roll. This is desirable because there is evidence that the upper roll tilts during its jumping motion at the higher speeds, making measurement at only one end inconclusive. This force measurement is being coupled with the present hydraulic force transducer to give an improved measurement of the instantaneous average hydraulic force. Alternatively, the measurements at either end of the upper roll can be recorded on separate dual-beam oscilloscopes if the motions of the two ends are to be studied independently.

From these measurements it is believed there will proceed (a) better estimates of the magnitude of the molding stress as a function of corrugator operation and medium properties, and (b) greater insight into the causes of highs-and-lows and leaning flutes in combined board and the factors which govern runnability.

THE INSTITUTE OF PAPER CHEMISTRY

J. W. Gander

J. W. Gander, Research Aide
Container Section

R. C. McKee

R. C. McKee, Chief
Container Section

LITERATURE CITED

1. The Institute of Paper Chemistry. Behavior of fibrous and nonfibrous components in the corrugating operation. Part I. Analysis of stress and strain in medium during formation of flutes. Progress Report One to Fourdrinier Kraft Board Institute, Inc., Project 1108-22, Feb. 29, 1960.

2. Anon. W-S flute design brings new concept of corrugating. Fibre Containers and Paperboard Mills 44, no. 4:69-72 (April, 1959).

3. Peters, W. Measuring forces that cause production problems in corrugated manufacture. Paperboard Packaging 46, no. 2:60-3 (Feb., 1961).

4. Report in preparation at The Institute of Paper Chemistry.

5. Thomson, W. J. Mechanical vibrations. p. 55, New York, Prentice-Hall, Inc., 1948.

6. Mauer, E. R., Roark, R. J., and Washa, G. W. Mechanics for engineers. p. 198, New York, John Wiley and Sons, Inc., 1945.

7. Reference (5), p. 5.

8. McKee, R. C. Corrugating variables and the effect on combined board characteristics. Tappi 43, no. 3:218A-28A (March, 1960).

APPENDIX A

SYMBOLS

F = resultant force exerted by bottom roll on upper roll, lb.

F_f = force of friction between guide rods and bearing assemblies, lb.

g = acceleration of gravity, 386 in./sec.^{2}

H = force exerted by hydraulic system on upper roll, lb.

H_d = dynamic component of hydraulic force, lb.

H_s = static component of hydraulic force, lb.

I = mass moment of inertia, lb. in. sec.^{2}

k_h = spring constant of hydraulic system, lb./in.

M_f = moment of friction due to rotary bearing friction of upper roll, lb.-in.

m = mass, W/g, lb. sec.^{2}/in.

R = radial component of force exerted by bottom roll on upper roll, lb.

R_d = dynamic component of radial force exerted by bottom roll, lb.

R_s = static component of radial force exerted by bottom roll, lb.

T = tangential component of force exerted by bottom roll on upper roll, lb.

t = time, sec.

W = weight of upper corrugating roll and bearing assembly, lb.

x = co-ordinate of displacement of upper roll parallel to the line joining the centers of the corrugating rolls, in.

$\dot{x} = dx/dt$ = velocity, in./sec.

$\ddot{x} = d^2x/dt^2$ = acceleration, in./sec.^{2}

β = angle between resultant force of bottom roll and line of roll centers, rad.

Δ = difference

APPENDIX A--Continued

SYMBOLS

θ = angle of rotation of upper corrugating roll about its axis of rotation, rad.

$\ddot{\theta} = d^2\theta/dt^2$ = angular acceleration of upper roll, rad./sec.^{2}

μ = coefficient of sliding friction, dimensionless

APPENDIX B

ERROR OF GRAPHICAL DETERMINATION OF ACCELERATION

An appreciation for the inherent error introduced by a graphical determination of acceleration from a displacement vs. time curve may be gained from consideration of a simple harmonic motion, $x = \sin t$, as diagrammed in Fig. 9. The origin of co-ordinates is taken at the right-hand side of the illustration in conformity with the oscilloscope traces of Fig. 6. That consideration of a simple sine curve is appropriate to this discussion, it may be recalled that any periodic motion can be approximated to an arbitrary degree of accuracy by a series of sine (or cosine) functions of progressively increasing frequency and that, furthermore, frequently the first harmonic term serves as a satisfactory first, though crude, approximation. The latter would appear to be true of the oscilloscope curves of Fig. 6.

For the sine function diagrammed in Fig. 9, the maximum acceleration, $\ddot{x}_2$, which occurs at point T, is given exactly by

$$\ddot{x}_2 = \left.\frac{d^2x}{dt^2}\right|_{t = \pi/2} = \left. - \sin t \right|_{t = \pi/2} = - 1.0 \qquad (18)$$

The velocity, $\dot{x}_1$, at any arbitrary point A is given by

$$\dot{x}_1 = \frac{dx}{dt} = \cos t \qquad (19)$$

and the velocity at T is

$$\dot{x}_2 = \left. \cos t \right|_{t = \pi/2} = 0. \qquad (20)$$

From Equations (19) and (20), the average acceleration from A to T is

$$\bar{\ddot{x}} = (\dot{x}_2 - \dot{x}_1) / \Delta t = - (\cos t) / \Delta t. \qquad (21)$$

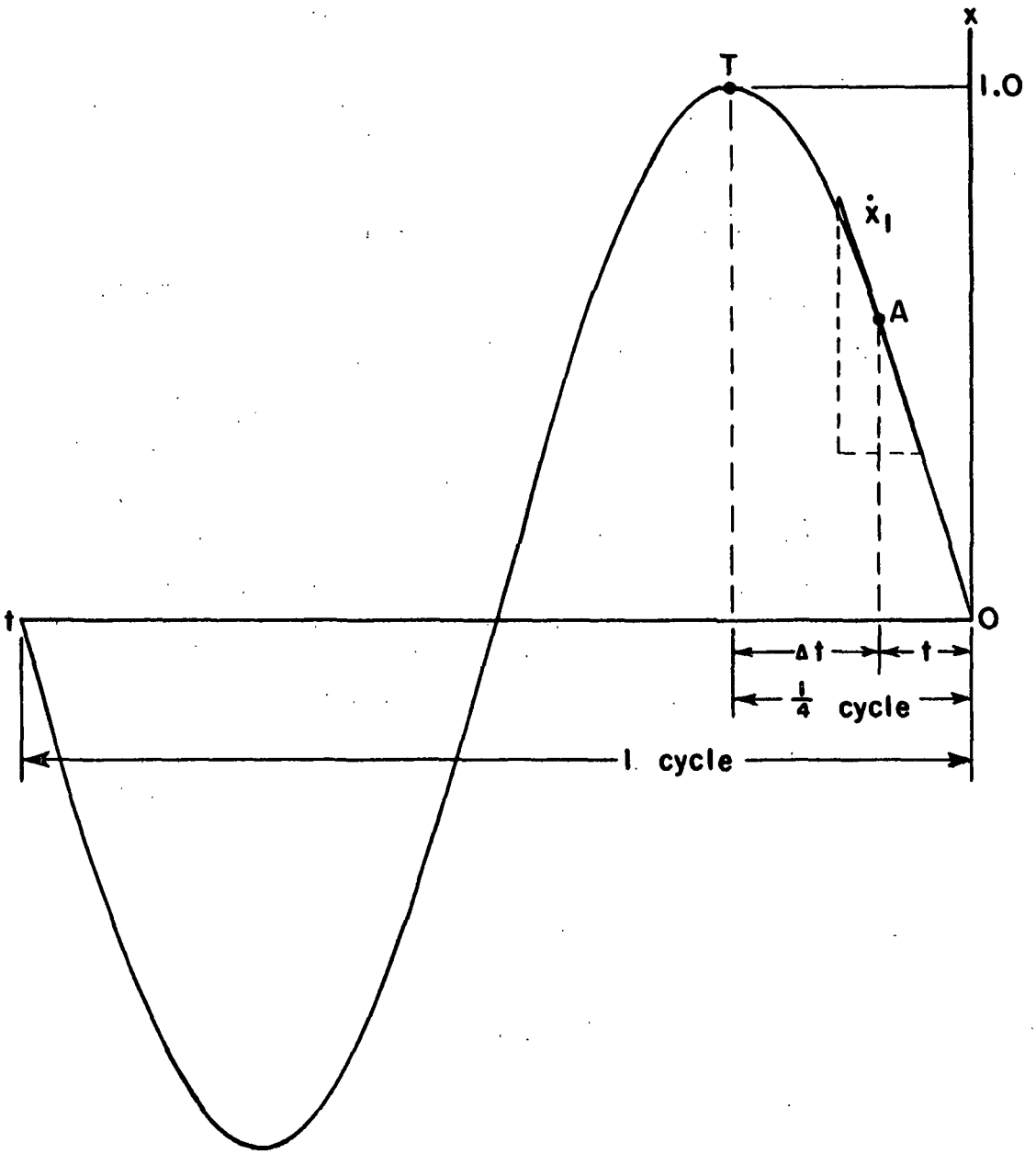

Figure 9. Displacement vs. Time Curve for Simple Harmonic Motion,

$x = \sin t$

The average acceleration obtained from Equation (21), for various points A, may be compared with the peak acceleration at point T for purposes of studying the inherent error of a graphical determination of acceleration. Computation of average acceleration and the aforementioned comparison are summarized in Table III.

It may be seen from the data of Table III that the difference between the average acceleration (as would be determined graphically) and the exact acceleration at the peak of the curve diminishes as the point A approaches the peak of the curve. At $t = 45°$, which is one-half of a quarter cycle, the average acceleration is 10% less than the peak acceleration. The maximum error is -36%, when point A is taken at the origin of the half-wave.

In projecting these results to the graphical determination of acceleration from a displacement-time curve such as Fig. 6, it must be remembered that the above considerations presume that the tangent at point A is drawn accurately and that the curve in question is approximated adequately by a sine function.

TABLE III

ERROR IN GRAPHICAL DETERMINATION OF ACCELERATION

FOR SIMPLE HARMONIC MOTION

Time, t, degrees	cos t	Δt radian	Average Acceleration, $\bar{x}$	Per Cent Difference from Peak Acceleration[a]
0	1.000	1.571	-0.637	-36.3
5	0.996	1.484	-0.672	-32.8
10	0.985	1.396	-0.707	-29.3
15	0.966	1.309	-0.740	-26.0
20	0.940	1.222	-0.770	-23.0
25	0.906	1.134	-0.799	-20.1
30	0.867	1.047	-0.829	-17.1
35	0.819	0.960	-0.853	-14.7
40	0.766	0.873	-0.879	-12.1
45	0.707	0.785	-0.900	-10.0
50	0.643	0.698	-0.922	- 7.8
55	0.574	0.611	-0.939	- 6.1
60	0.500	0.524	-0.955	- 4.5
65	0.423	0.436	-0.970	- 3.0
70	0.342	0.349	-0.980	- 2.0
75	0.259	0.262	-0.989	- 1.1
80	0.174	0.175	-0.995	- 0.5
85	0.087	0.087	-0.999	- 0.1
90	0.000	0.000	--	--

[a] Peak acceleration is negative unity at $t = 90°$.